Clays and Clay Minerals, Vol. 48, No. 5, 503–510, 2000.

EFFECT OF PHOSPHATE ON THE FORMATION OF NANOPHASE LEPIDOCROCITE FROM Fe(II) SULFATE

JESÚS CUMPLIDO, VIDAL BARRÓN, AND JOSÉ TORRENT

Departamento de Ciencias y Recursos Agrícolas y Forestales, Universidad de Córdoba, Apdo. 3048, 14080 Córdoba, Spain

Abstract—The effect of phosphate on the formation of Fe oxides from Fe(II) salts is important because phosphate is a ubiquitous anion in natural environments. For this reason, the products formed by oxidation of phosphate-containing $Fe(II)SO_4$ solutions neutralized with bicarbonate were characterized. The rate of oxidation of Fe(II) increased with increasing P/Fe atomic ratio to 0.2 in the initial solution. Goethite (α-FeOOH) or lepidocrocite (γ-FeOOH) or both were produced and identified by powder X-ray diffraction (XRD). The ratio between lepidocrocite and goethite increased with increasing P/Fe. In the 5–8.5 pH range, the formation of goethite predominated at P/Fe < 0.005, but only lepidocrocite was detected by XRD for P/Fe > 0.02. Thus, phosphate favors lepidocrocite formation because lepidocrocite has (1) a layered structure (like its precursor green rust), and (2) a structure less dense than that of goethite, thereby requiring less complete removal of the green-rust interlayer phosphate to form. The lepidocrocite crystals were platy, with prominent {010} faces and the thickness of the plates decreased with increasing P/Fe from >25 nm for P/Fe < 0.005 to <5 nm for P/Fe > 0.1. The solubility of lepidocrocite in acid oxalate was nearly complete for P/Fe > 0.03. The lepidocrocite contained occluded phosphate, *i.e.*, phosphate that could not be desorbed by alkali treatment. The decrease in the *b* unit-cell length with increasing P/Fe suggests that lepidocrocite may contain structural P.

Key Words—Goethite, Lepidocrocite, Nanophase, Phosphate, Rietveld Analysis.

INTRODUCTION

The formation of Fe oxides (a term used here to include iron oxides and oxyhydroxides) from Fe salts, whether in natural environments or in the laboratory, is influenced by Fe concentration, pH, temperature, foreign compounds, and other factors (Cornell and Schwertmann, 1996). In particular, phosphate affects strongly the degree of transformation of Fe(III) salts, as well as the morphological properties, and phosphorus (P) content of the resulting crystalline Fe oxides (Reeves and Mann, 1991; Morales *et al.*, 1992; Ocaña *et al.*, 1995; Sugimoto and Muramatsu, 1996; Barrón *et al.*, 1997; Gálvez *et al.*, 1999a, 1999b). For example, some hematites prepared from Fe(III) salts in the presence of phosphate contain P that cannot be desorbed after several alkali treatments, perhaps suggesting that the P is structural (Gálvez *et al.*, 1999b).

The effect of phosphate on the formation of Fe oxides from Fe(II) salts has received scant attention, probably because no crystalline oxides were formed in experiments where the ratio of P to Fe was large (Detournay *et al.*, 1975). However, small amounts of some anions like phosphate that are adsorbed by ligand exchange (*e.g.*, sulfate, carbonate, silicate, and citrate) do not prevent crystallization of Fe oxides (Cornell and Schwertmann, 1996; Liu and Huang, 1999). Therefore, by analogy, small amounts of phosphate may not prevent crystallization of Fe oxides either. This hypothesis is consistent with the presence of crystalline Fe oxides in many natural environments (*e.g.*, soils) where phosphate occurs in significant amounts. Phosphate would be expected to influence the type and properties of the crystalline oxide formed, as is the case with the anions given above (Cornell and Schwertmann, 1996; Liu and Huang, 1999).

Phosphate is a ubiquitous solute in aquatic environments. Understanding its role in the formation of Fe oxides via hydrolysis and oxidation of Fe(II) solutions would be useful in explaining and predicting chemical and mineralogical changes occurring in these environments. For instance: (1) Chemical reduction in flooded soils usually results in the production of high concentrations of Fe(II) and phosphate in solution resulting from dissolution of Fe oxides and the release of adsorbed phosphate (Ponnamperuma, 1972). The phosphate concentration in the soil solution may likely affect the type of Fe oxide formed on reoxidation and, consequently, the future phosphate adsorption behavior of the soil (de Mello *et al.*, 1998). (2) The effectiveness of synthetic vivianite [$Fe_3(PO_4)_2 \cdot 8H_2O$] and other Fe(II) phosphates in correcting Fe deficiency in plants grown in calcareous soils was attributed to the oxidation and incongruent dissolution of these compounds, which are likely to yield Fe oxides of large specific surface area and high solubility (Eynard *et al.*, 1992). Characterizing the effect of phosphate on these reactions would enhance the use of these P- and Fe-rich fertilizers.

The objective of this paper, therefore, was to examine the influence of phosphate on the type, morphology, and properties of iron oxides synthesized by hydrolysis and oxidation of Fe(II) sulfate.

MATERIALS AND METHODS

Solutions of 0.05 M $FeSO_4 \cdot 7H_2O$ and 0.01 M KH_2PO_4 were mixed in the P/Fe atomic ratio range of

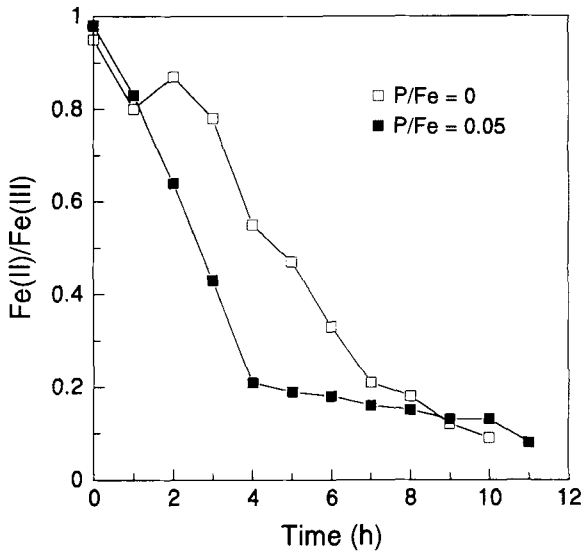

Figure 1. Effect of time on the Fe(II)/Fe(III) ratio in the green-rust suspension at pH 7 for P/Fe = 0 and 0.05.

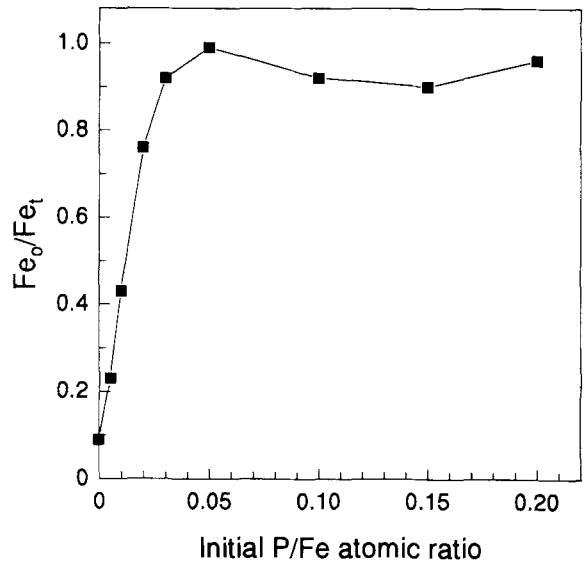

Figure 2. The Fe_o/Fe_t ratio of the solid products synthesized at pH 7 as a function of the initial P/Fe ratio.

0–0.2. The initial solutions were brought to the desired pH of 5.5, 7, and 8.5 with 1 M $NaHCO_3$. To keep a constant pH during hydrolysis and oxidation of Fe(II), a pH stat was required at pH 5.5 but not at pH 7 or 8.5. The oxidation of the initial green-rust precipitate was performed in open vessels by bubbling air at a flow rate of 30–40 mL min^{-1} into 500 mL of the continously stirred suspension. Oxidation was complete within 48 h, during which time the color of the suspension changed from green-blue to ochre. Then, the solid products were washed with water by repeatedly centrifuging the suspension and decanting the supernatant and, finally, dialyzed in deionized water until the electrical conductivity of the equilibrium solution was <1 mS m^{-1}. The resulting slurry was suspended in 100 mL of deionized water.

Oxalate-soluble Fe (Fe_o) was determined by dissolving the products in 0.2 M NH_4-oxalate with pH of 3 for 2 h in the dark (Schwertmann, 1964). Total Fe and P (Fe_t, P_t) and Fe(II) were determined by dissolving 1 mL of the suspension in 1 mL of cold 11 M HCl. The NaOH-extractable P (P_{NaOH}) was determined by shaking a portion of the oxide suspension in 50 mL of 0.1 M NaOH at 298 K for 16 h. In all extracts, P was determined by the molybdenum-blue method of Murphy and Riley (1962) and Fe_t and Fe(II) by the o-phenanthroline method (Olson and Ellis, 1982), except that no hydroxylamine was used in the determination of Fe(II).

Samples of the dialyzed products were dried in an oven at 313 K. Powder X-ray diffraction (XRD) patterns were obtained with a Siemens D5000 diffractometer equipped with CoKα radiation and a graphite monochromator at a step size of 0.02 °2θ and a counting time of 10 s. Phase and crystal parameters were calculated by fitting the XRD scans to the Rietveld equation (Rietveld, 1967) with the GSAS computer program (Larson and Von Dreele, 1988). The structural parameters included in the refinement were those given by Oles *et al.* (1970) for lepidocrocite and by Forsyth *et al.* (1968) for goethite. The lepidocrocite/

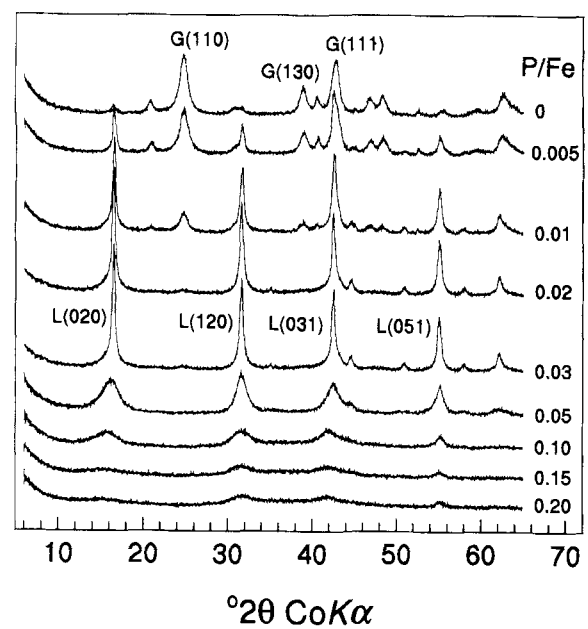

Figure 3. X-ray diffraction patterns of the products synthesized at pH 7 as a function of the P/Fe ratio in the initial solution. The most characteristic goethite (G) and lepidocrocite (L) reflections are labeled.

https://doi.org/10.1346/CCMN.2000.0480502 Published online by Cambridge University Press

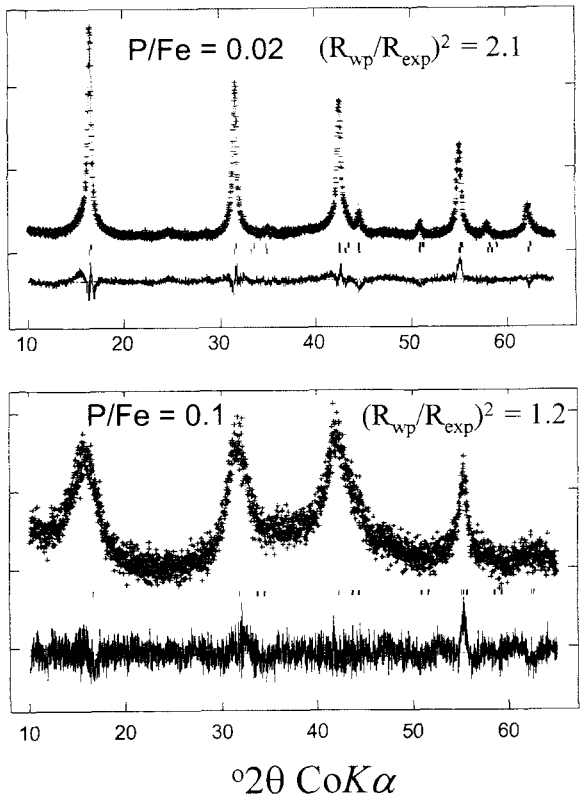

Figure 4. Observed (+) and calculated (solid line) X-ray powder diffraction data for samples synthesized at P/Fe = 0.02 (upper) and P/Fe = 0.10 (lower). In each box, the lower curve is the difference between observed and calculated profiles.

goethite ratio was calculated as detailed by Weidler *et al.* (1998).

Transmission electron microscope (TEM) specimens of the products were prepared by depositing a drop of the dilute aqueous suspension on C-coated Formvar film supported by a copper grid, which was then examined with a Jeol JEM-200CX instrument. Observation by atomic force microscopy (AFM) involved particles mounted on a muscovite surface and a Multimode Scanning Probe Microscope (Digital Instruments, Santa Barbara, California, USA). To avoid artifacts from the probe, tapping mode with an etched-silicon probe (solid angle between 20–50°) was used (Barrón *et al.*, 1997).

Diffuse-reflectance spectra of powder mounts were obtained with a Varian Cary 1E spectrophotometer. The reflectance (R) values were taken at intervals of 0.5 nm in the 380–710 nm range and converted to the Munsell color parameters (Barrón and Torrent, 1986). The second-derivative curve of the Kubelka-Munk function $[(1 - R)^2/2R]$ was obtained as described by Scheinost *et al.* (1998). Infrared (IR) spectra of KBr pellets (0.5 wt. % sample) were recorded from 380 to 4000 cm^{-1} with a Perkin-Elmer 2000 FTIR spectrometer using 4 cm^{-1} resolution and an average of 100 scans.

The specific surface area and the micropore surface area were determined by N_2 adsorption using the BET method and the t-plot method, respectively, as described by Webb and Orr (1997). A Micromeritics ASAP 2010 surface area analyzer (Micromeritics Instrument Corporation, Norcross, Georgia, USA) was used for this purpose.

RESULTS

Effect of phosphate on the oxidation and transformation of green rust

The initial rate of oxidation of the green rust increased with increasing P/Fe, as illustrated in Figure 1for the products obtained at pH 7 for the ratios of P/Fe of 0 and 0.05. This result is consistent with previous observations that phosphate is an anion that accelerates the rate of oxidation of Fe(II) in aqueous solutions (Tamura *et al.*, 1976).

The Fe_o/Fe_t ratio increased sharply with increasing P/Fe (Figure 2). On the basis of the oxalate test, the products synthesized in absence of P were crystalline ($Fe_o/Fe_t < 0.1$), whereas poorly crystalline products ($Fe_o/Fe_t > 0.9$) predominated at P/Fe > 0.03.

Morphology and properties of the products

According to Schwertmann and Cornell (1991), lepidocrocite is not formed in significant amounts when the HCO_3/Fe mole ratio is 1.5–2 (as it was in our experiments). So, goethite and only traces of lepidocrocite were identified by XRD in the sample synthesized at pH 7 in the absence of phosphate (Figure 3). With increasing P/Fe, the goethite-promoting effect of HCO_3 relative to systems without this ion (Carlson and Schwertmann, 1990) was gradually suppressed, so lepidocrocite and only traces of goethite were detected for P/Fe = 0.02 in the initial solution. Phosphate also suppressed the effect that sulfate has in favoring goethite over lepidocrocite (Carlson and Schwertmann, 1990; Frini and Elmaaoui, 1997).

Between P/Fe of 0.03–0.2, the XRD reflections of lepidocrocite became increasingly broader with increasing P/Fe (Figure 3), indicating decreasing domain size or increasing crystalline disorder or strain in the crystal. At P/Fe = 0.2, very broad lepidocrocite (020), which is weak, and (120), (031), and (051) reflections were observed. Similar results were obtained for pH 5.5 and 8.5 (not shown), suggesting that within the 5.5–8.5 range, pH has little effect on the properties of lepidocrocite formed in the presence of phosphate. Consequently, only the properties of the products formed at pH 7 will be described below.

The fitting by Rietveld analysis of the diffractograms of the products was "good", as suggested by the value of the $(R_{wp}/R_{exp})^2$ parameter (Bish, 1993),

https://doi.org/10.1346/CCMN.2000.0480502 Published online by Cambridge University Press

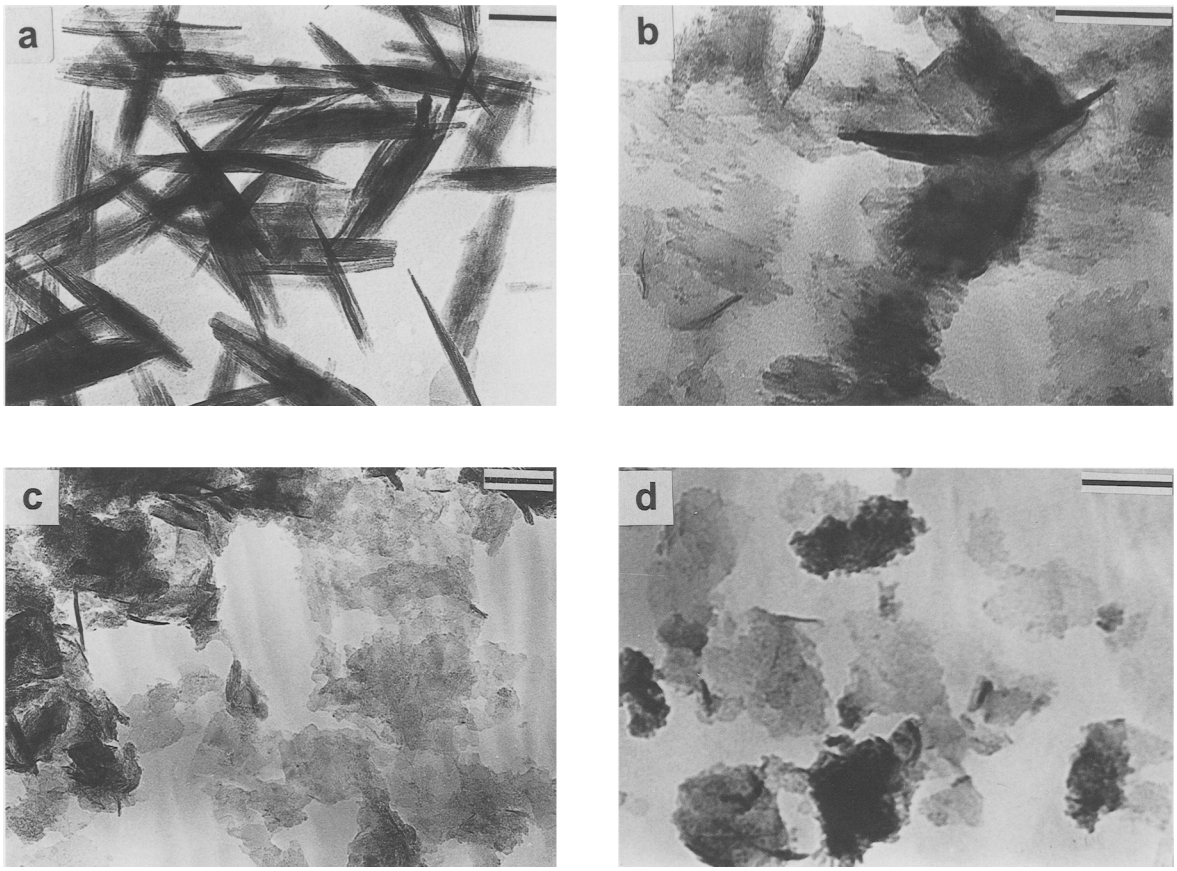

Figure 5. Transmission electron micrographs of the products synthesized at pH 7. (a) Goethite synthesized at P/Fe = 0. (b) Lepidocrocite synthesized at P/Fe = 0.02. (c) Lepidocrocite synthesized at P/Fe = 0.05. (d) Lepidocrocite synthesized at P/Fe = 0.15. Bars are 100 nm.

Table 1. Properties of the products.

[1]P/Fe	[2]Mineralogical composition	Fe_r/Fe_i	Rietveld-analysis [3]L/(L + G)	Rietveld-analysis [4]$(R_{wp}/R_{ex})^2$	[5]Unit-cell edge lengths of lepidocrocite *a* (nm)	*b* (nm)	*c* (nm)	[6]MCL (nm)	Length × width (TEM) (nm)	Specific surface area ($m^2\ g^{-1}$)	Microporosity ($m^2\ g^{-1}$)	Munsell color
0.00	G + L	0.09	0.03	2.1	—	—	—	—	[7]300 × 40	88	28	7.4YR 5.0/6.2
0.005	G + L	0.23	0.21	2.2	0.3058(1)	1.2524(8)	0.3866(1)	26	—	108	3	7.0YR 4.6/7.0
0.01	G + L	0.43	0.61	1.9	0.3062(1)	1.2504(3)	0.3865(1)	20	—	112	0	6.1YR 4.5/6.9
0.02	L	0.76	~1.00	2.1	0.3067(1)	1.2500(3)	0.3867(1)	20	[7]100 × 70	127	0	5.4YR 4.4/6.5
0.03	L	0.92	~1.00	1.7	0.3067(1)	1.2495(4)	0.3866(1)	13	—	155	0	5.4YR 4.3/7.1
0.05	L	0.99	1.00	1.6	0.3078(2)	1.240(1)	0.3856(1)	9	[7]15–70	198	0	5.0YR 3.9/7.0
0.10	L + F(?)	0.92	1.00	1.2	0.3113(3)	1.232(1)	0.3836(2)	5	—	254	0	4.4YR 3.5/5.9
0.15	L + F(?)	0.90	1.00	—	—	—	—	—	—	260	2	5.4YR 4.4/7.0
0.20	L + F(?)	0.96	1.00	—	—	—	—	—	—	245	3	5.1YR 4.4/7.5

[1] P/Fe atomic ratio of the initial solution.
[2] G = goethite; L = lepidocrocite; F = ferrihydrite.
[3] Lepidocrocite/(lepidocrocite + goethite) ratio in the final products.
[4] Index of goodness of fit (Bish, 1993). R_{wp} = weighted profile residual; R_{ex} = expected residual; for perfect refinement, $(R_{wp}/R_{ex})^2 = 1$.
[5] Standard deviations in brackets are in units of least significant figure of main value. Unit cell lengths for the *Cmcm* space group.
[6] Mean coherence length in the *b* direction.
[7] Acicular, tabular, and platy, respectively.

https://doi.org/10.1346/CCMN.2000.0480502 Published online by Cambridge University Press

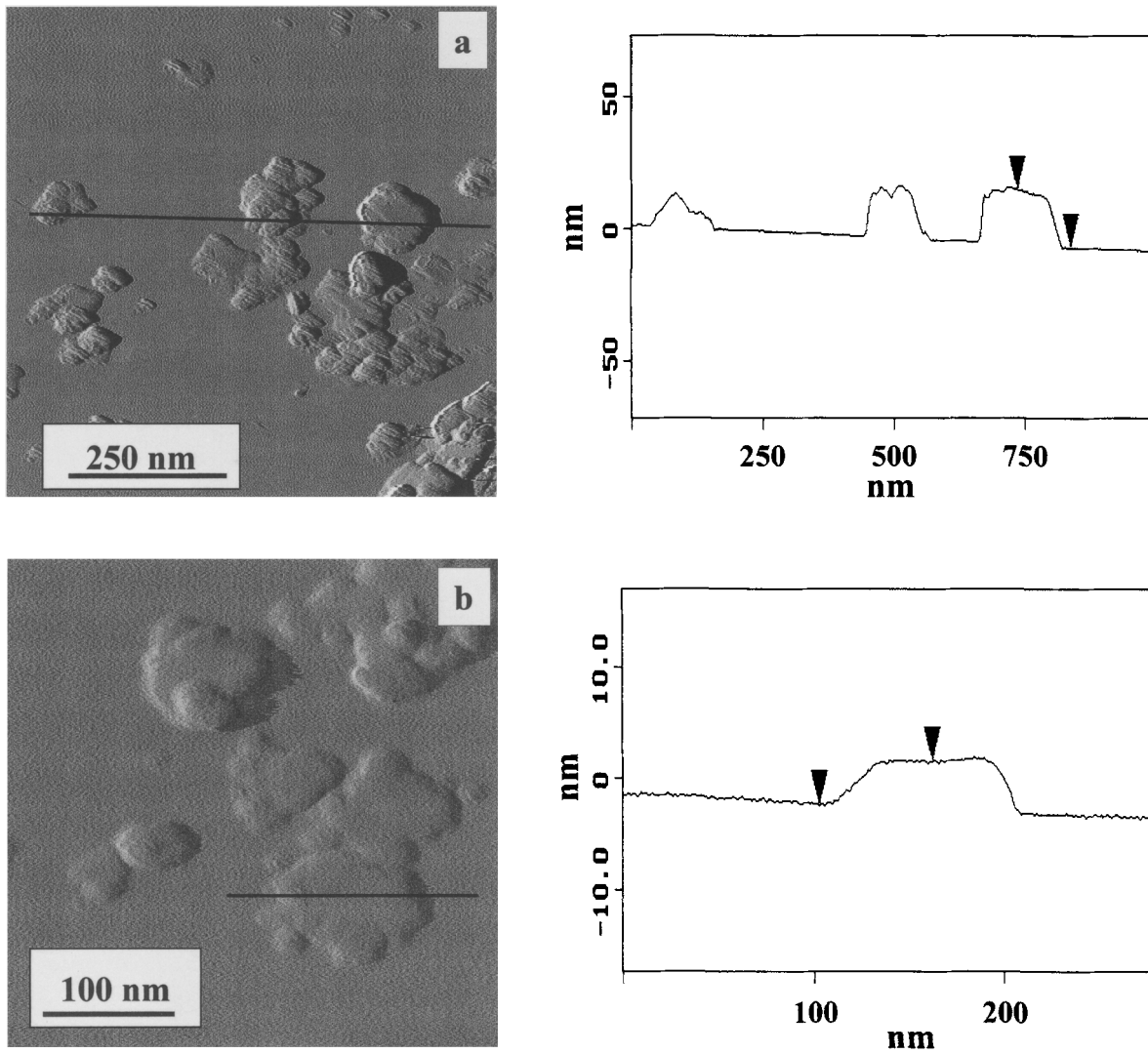

Figure 6. AFM images of the lepidocrocite synthesized at P/Fe = 0.02 (a) and P/Fe = 0.05 (b). Each cross section corresponds to the line marked on the image to the left.

which ranged from 1.2 to 2.2 (Table 1). Figure 4 shows the results of the Rietveld analysis for the two products containing only lepidocrocite and showing the extreme $(R_{wp}/R_{exp})^2$ values. The estimated lepidocrocite/(lepidocrocite + goethite) ratio and the crystalline parameters of lepidocrocite are given in Table 1. The unit-cell lengths of lepidocrocite changed with P/Fe, suggesting that structural P is present in lepidocrocite formed in the presence of phosphate. Mean coherence length (MCL) in the [010] direction of lepidocrocite, estimated from the Lorentzian broadening obtained in the Rietveld analysis, decreased to very small values (<10 nm, nanophase lepidocrocite) for P/Fe ≥ 0.05.

The TEM images of the samples synthesized at P/Fe = 0.02, 0.05, and 0.15 (Figure 5) showed platy lepidocrocite crystals with prominent {010} faces, as is usually observed for this mineral. The particle width ranged from 15 to 100 nm. Particle thickness, estimated by AFM, was ~20 and ~4 nm for the samples prepared at P/Fe = 0.02 and 0.05, respectively (Figure 6). The latter value indicates that lepidocrocite crystals (b = 1.24 nm) have layers of three unit cells. The specific surface area increased from 90 to ~250 m^2 g^{-1} with increasing P/Fe (Table 1). This is consistent with the small size of the lepidocrocite particles and also with the possible presence of ferrihydrite.

Note that the small size of the lepidocrocite crystals, particularly for the samples synthesized at P/Fe > 0.01, may explain the high solubility of the samples in oxalate; indeed, lepidocrocite of 116 m^2 g^{-1} was almost 80% soluble in oxalate (Reyes and Torrent,

https://doi.org/10.1346/CCMN.2000.0480502 Published online by Cambridge University Press

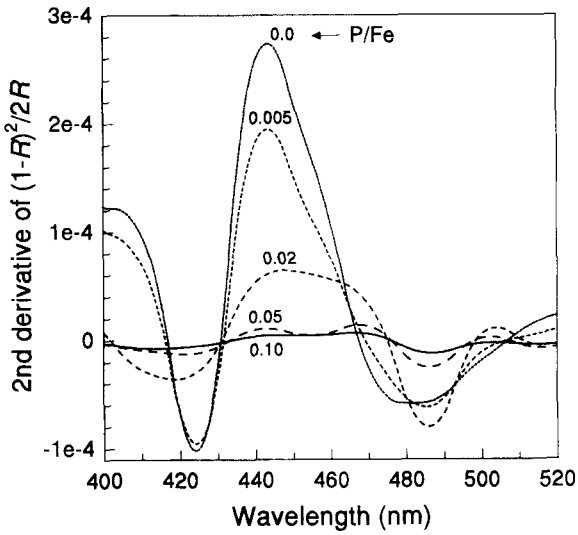

Figure 7. Second-derivative curves of the Kubelka-Munk function $[(1 - R)^2/2R]$ of the products synthesized at different P/Fe ratios.

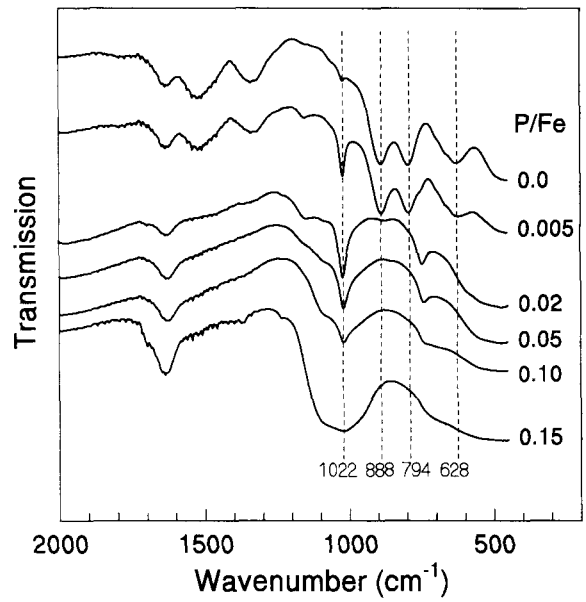

Figure 8. Infrared spectra of the products synthesized at different P/Fe ratios.

1997). So, it is difficult to estimate the relative proportions of ferrihydrite (if any) and lepidocrocite in the samples. The proportion of ferrihydrite is probably small, given that the samples have a surface area in micropores of ≤ 3 m^2 g^{-1} (Table 1). This value is much smaller than the value expected for ferrihydrite (>200 m^2 g^{-1}; Weidler, 1995).

Spectral properties

The Munsell color of the samples prepared at pH 7 ranged from 7.4YR 5.0/6.2 to 5.1YR 4.4/7.5 (Table 1). Generally, with increasing P/Fe (and lepidocrocite content), the color became redder and darker. This might be due to the decreasing size of the lepidocrocite crystals (Schwertmann, 1993). Differences in color cannot be exclusively attributed to the nature of the crystalline products, as small amounts of ferrihydrite might be present in some samples. The second-derivative curve of the diffuse reflectance spectra (Figure 7) showed two minima (corresponding to absorption bands) at 420–425 and 480–485 nm. The position of the bands was not related to the P/Fe ratio but their intensities decreased steadily with increasing P/Fe. This indicates that (1) lepidocrocite shows weaker absorption bands than goethite, as was found by Scheinost *et al.* (1998), and (2) that the lepidocrocite bands are sensitive to particle size and shape.

The IR absorption spectra (Figure 8) show the typical 628, 794, and 888 cm^{-1} goethite bands and two carbonate bands (~1340 and ~1510 cm^{-1}) for the P-free sample. With increasing P/Fe, the vibration bands for lepidocrocite (~750 and ~1022 cm^{-1}) occur. The broadening of the 1022-cm^{-1} band for lepidocrocite is probably related to the overlapping of the P–O(H) stretching vibrations in the 970–1040 cm^{-1} range (Gálvez *et al.*, 1999b).

Forms of phosphate associated with the products

An ~1:1 relation existed between the P/Fe in most products of the synthesis and the P/Fe in the initial solution. This indicates that essentially all the phosphate was associated with the solid products. After treating the solid products with NaOH, which removes

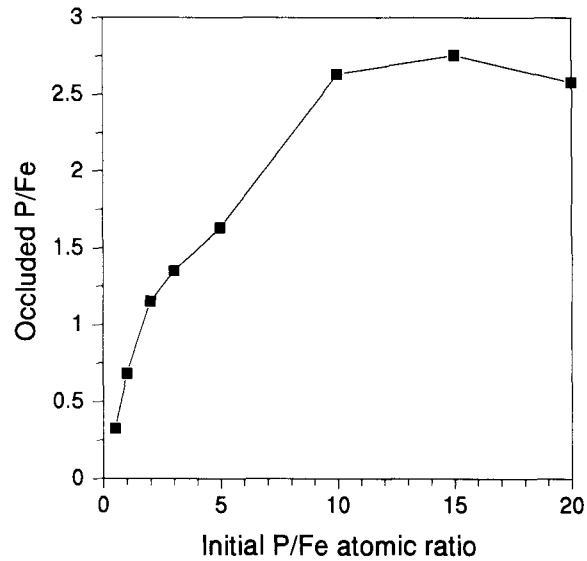

Figure 9. Relationship between the ratio of occluded (non-hydroxyl-extractable) P and Fe in the solid products and the P/Fe ratio in the initial solution.

https://doi.org/10.1346/CCMN.2000.0480502 Published online by Cambridge University Press

the phosphate adsorbed on the surface of the Fe oxides (Cabrera *et al.,* 1981), significant amounts of P remained in the solid phases. Figure 9 shows that the ratio between the amount of the non-hydroxyl-extractable P (which can be denoted as "occluded" P) and Fe in the solids increased with the P/Fe ratio in the initial solution. The curve in Figure 9 reaches a plateau for an initial P/Fe ratio of ~0.10, where the ratio of occluded P to Fe is ~0.026.

DISCUSSION

Green rusts (GRs) have the ideal composition $[Fe^{2+}_{(6-x)}\ Fe^{3+}_{x}(OH)_{12}][(A_{x/n})\cdot yH_2O]$, where A^{n-} is an n-valent anion that occurs in the interlayer between sheets of hexagonally closest-packed Fe(II)Fe(III) octahedra. GRs are capable of adsorbing phosphate by exchanging a portion of interlayer anions (Hansen and Poulsen, 1999). Our experiments show that interlayer phosphate favors the transformation of GR into lepidocrocite and not goethite. One possible reason for the formation of lepidocrocite is that crystallization of the more dense structure of goethite requires removal of the interlayer phosphate ions. In contrast, lepidocrocite is both less dense and, like GR, has a layered structure. Therefore, lepidocrocite may be formed without complete removal of the interlayer phosphate from the precursor GR.

Phosphate increased the rate of oxidation of Fe(II) (Figure 1). Cornell and Schwertmann (1996) reported that rapid oxidation favors formation of lepidocrocite *versus* goethite from Fe(II) salts. However, the rate of Fe(II) oxidation does not seem to be a critical factor in determining lepidocrocite over goethite formation, given that anions that retard oxidation (*e.g.,* citrate and silicate) also favor lepidocrocite formation (Krishnamurti and Huang, 1991, 1993, 1998; Liu and Huang, 1999).

This work has shown that lepidocrocite can accommodate phosphate in a non-hydroxyl-extractable, occluded P form, as was the case with hematite (but not goethite) produced from Fe(III) salts (Gálvez *et al.,* 1999a, 1999b). The *b* unit-cell length is negatively correlated with the ratio of occluded P to Fe in the solid products [$b = 1.2576 - 0.912 \times$ (occluded P/Fe); $R^2 = 0.865$; $p < 0.01$]. Such observed reduction in *b* suggests that this occluded P may be structural phosphate possibly substituting for OH in the lepidocrocite structure.

Dissolution in oxalate was nearly complete for samples in which the lepidocrocite plates were <20 nm in mean thickness according to AFM measurements. Oxalate treatment does not allow the separation of P-doped, nanophase lepidocrocite from ferrihydrite, thereby making it difficult to identify and quantify nanophase lepidocrocite in the environments where it may occur. The high solubility and specific surface area of lepidocrocite formed in the presence of phosphate provides a plausible explanation for the effectiveness of vivianite and other Fe(II) phosphates as Fe fertilizers (Eynard *et al.,* 1992), because there is some evidence that some nanophase lepidocrocite can be produced by oxidation and incongruent dissolution of these phosphates (Barrón and Torrent, unpublished data).

ACKNOWLEDGMENTS

This work was supported by the C.I.C.Y.T. of Spain under Projects OLI96-2183 and PB98-1015.

REFERENCES

Barrón, V. and Torrent, J. (1986) Use of the Kubelka-Munk theory to study the influence of iron oxides on soil color. *Journal of Soil Science,* **37,** 499–510.

Barrón, V., Gálvez, N., Hochella, M.F., Jr., and Torrent, J. (1997) Epitaxial overgrowth of goethite on hematite synthesized in phosphate media: A scanning force and transmission electron microscopy study. *American Mineralogist,* **82,** 1091–1100.

Bish, D.L. (1993) Studies of clays and clay minerals using X-ray powder diffraction and the Rietveld method. In *Computer Applications to X-ray Diffraction Analysis of Clay Minerals,* R.C. Reynolds and J.R. Walker, eds., The Clay Mineral Society, Boulder, Colorado, 79–121.

Cabrera, F., de Arambarri, P., Madrid, L., and Toca, C.G. (1981) Desorption of phosphate from iron oxides in relation to equilibrium pH and porosity. *Geoderma,* **26,** 203–216.

Carlson, L. and Schwertmann, U. (1990) The effect of CO_2 and oxidation rate on the formation of goethite versus lepidocrocite from an Fe(II) system at pH 6 and 7. *Clay Minerals,* **25,** 65–71.

Cornell, R.M. and Schwertmann, U. (1996) *The Iron Oxides.* VCH, Weinheim, 573 pp.

de Mello, J.W.V., Barrón, V., and Torrent, J. (1998) Phosphorus and iron mobilization in flooded soils from Brazil. *Soil Science,* **163,** 122–132.

Detournay, J., Ghodsi, M., and Derie, R. (1975) Influence de la température et de la présence des ions etrangers sur la cinétique et le mécanisme de la formation de la goethite en milieu aqueux. *Zeitschrift für Anorganische und Allgemeine Chemie,* **412,** 184–192.

Eynard, A., del Campillo, M.C., Barrón, V., and Torrent, J. (1992) Use of vivianite ($Fe_3(PO_4)_2\cdot 8H_2O$) to prevent iron chlorosis in calcareous soils. *Fertilizer Research,* **31,** 61–67.

Forsyth, J.B., Hedley, J.G., and Johnson, C.E. (1968) The magnetic structure and hyperfine field of goethite (α-FeOOH). *Journal of Physics C,* **1,** 179–188.

Frini, A. and Elmaaoui, M. (1997) Kinetics of the formation of goethite in the presence of sulfates and chlorides on monovalent cations. *Journal of Colloid and Interface Science,* **190,** 269–277.

Gálvez, N., Barrón, V., and Torrent, J. (1999a) Effect of phosphate on the crystallization of hematite, goethite, and lepidocrocite from ferrihydrite. *Clays and Clay Minerals,* **47,** 304–311.

Gálvez, N., Barrón, V., and Torrent, J. (1999b) Preparation and properties of hematite with structural phosphorus. *Clays and Clay Minerals,* **47,** 375–385.

Hansen, H.C.B. and Poulsen, I.F. (1999) Interaction of synthetic sulphate "green rust" with phosphate and the crystallization of vivianite. *Clays and Clay Minerals,* **47,** 312–318.

Krishnamurti, G.S.R. and Huang, P.M. (1991) Influence of citrate on the kinetics of Fe(II) oxidation and the formation

of iron oxyhydroxides. *Clays and Clay Minerals,* **39,** 28–34.

Krishnamurti, G.S.R. and Huang, P.M. (1993) Formation of lepidocrocite from iron(II) solutions: Stabilization by citrate. *Soil Science Society of America Journal,* **57,** 861–867.

Krishnamurti, G.S.R. and Huang, P.M. (1998) The influence of pH and silicic acid concentration on Fe(II) transformations. *16th World Congress of Soil Science, Summaries, Volume I,* A. Ruellan, ed., ISSS-AFES, Montpellier, France, 445.

Larson, A.C. and Von Dreele, R.B. (1988) *GSAS. Generalized structure analysis system: Los Alamos National Laboratory Report LAUR 86-748.* Los Alamos National Laboratory, New Mexico, 150 pp.

Liu, C. and Huang, P.M. (1999) Properties of iron oxides formed at various citrate concentrations. In *Clays for Our Future. Proceedings of the 11th International Clay Conference, Ottawa, Canada 1997,* H. Kodama, A.R. Mermut, and J.K. Torrance, eds., ICC97 Organizing Committee, Ottawa, Canada, 513–522.

Morales, M.P., González-Carreño, T., and Serna, C.J. (1992) The formation of α-Fe_2O_3 monodispersed particles in solution. *Journal of Materials Research,* **7,** 2538–2545.

Murphy, J. and Riley, J.A. (1962) A modified single solution method for the determination of phosphate in natural waters. *Analitica Chimica Acta,* **27,** 31–36.

Ocaña, M., Morales, M.P., and Serna, C.J. (1995) The growth mechanism of α-Fe_2O_3 ellipsoidal particles in solution. *Journal of Colloid and Interface Science,* **171,** 85–91.

Oles, A., Szytula, A., and Wanic, A. (1970) Neutron diffraction study of γ-FeOOH. *Physica Status Solidi,* **41,** 173–177.

Olson, R.V. and Ellis, R., Jr. (1982) Iron. In *Methods of Soil Analysis, Part 2, 2nd edition,* A.L. Page, R.H. Miller, and D.R. Keeney, eds., American Society of Agronomy and Soil Science Society of America, Madison, Wisconsin, 301–312.

Ponnamperuma, F.N. (1972) The chemistry of submerged soils. *Advances in Agronomy,* **24,** 29–96.

Reeves, N.J. and Mann, S. (1991) Influence of inorganic and organic additives on the tailored synthesis of iron oxides. *Journal of the Chemical Society Faraday Transactions,* **87,** 3875–3880.

Reyes, I. and Torrent, J. (1997) Citrate-ascorbate as a highly selective extractant for poorly crystalline iron oxides. *Soil Science Society of America Journal,* **61,** 1647–1654.

Rietveld, H.M. (1967) Line profiles of neutron powder-diffraction peaks for structure refinement. *Acta Crystallographica,* **22,** 151–152.

Scheinost, A.C., Chavernas, A., Barrón, V., and Torrent, J. (1998) Use and limitations of second-derivative diffuse reflectance spectroscopy in the visible to near-infrared range to identify and quantify Fe oxides in soils. *Clays and Clay Minerals,* **46,** 528–537.

Schwertmann, U. (1964) Differenzierung der Eisenoxide des Bodens durch Extraktion mit Ammoniumoxalat-Lösung. *Zeitschrift für Pflanzenernährung, Düngung und Bodenkunde,* **105,** 194–202.

Schwertmann, U. (1993) Relations between iron oxides, soil color, and soil formation. In *Soil Color,* J.M. Bigham and E.J. Ciolkosz, eds., Soil Science Society of America, Madison, Wisconsin, 51–69.

Schwertmann, U. and Cornell, R.M. (1991) *Iron Oxides in the Laboratory.* VCH, Weinheim, 137 pp.

Sugimoto, T. and Muramatsu, A. (1996) Formation mechanism of monodispersed Fe_2O_3 particles in dilute $FeCl_3$ solutions. *Journal of Colloid and Interface Science,* **184,** 626–638.

Tamura, H., Goto, K., and Nagayama, M. (1976) Effect of anions on the oxygenation of ferrous ion in neutral solutions. *Journal of Inorganic and Nuclear Chemistry,* **38,** 113–117.

Webb, P.A. and Orr, C. (1997) *Analytical Methods in Fine Particle Technology.* Micromeritics Instrument Corporation, Norcross, Georgia, 301 pp.

Weidler, P.G. (1995) Oberflächen und Porositäten synthetischer Eisenoxide. Ph.D. thesis, Technische Universität München, München, Germany, 141 pp.

Weidler, P.G., Luster, J., Schneider, J., Sticher, H., and Gehring, A.U. (1998) The Rietveld method applied to the quantitative mineralogical and chemical analysis of a ferralitic soil. *European Journal of Soil Science,* **49,** 95–105.

E-mail of corresponding author: cr1tocaj@uco.es

(Received 7 December 1999; accepted 16 April 2000; Ms. 406: A.E. Helge Stanjek)